Experimental Evidence for the Coexistence of Oscillatory and Steady States in the Peroxidase–Oxidase Reaction

Baltazar D. Aguda,* Lise-Lotte Hofmann Frisch, and Lars Folke Olsen

Contribution from the Biochemistry Institute, Odense University, Campusvej 55, DK-5230 Odense M, Denmark. *Received November 30, 1989*

Abstract: Experiments are reported that demonstrate the coexistence of periodic oscillations and a stable steady state in the aerobic oxidation of NADH catalyzed by horseradish peroxidase. This coexistence was generally observed when the enzyme concentration is low, typically around 0.5 μM. In agreement with the predictions of the computer simulations performed by Aguda and Larter (*J. Am. Chem. Soc.* **1990**, *112*, 2167–2174), it was observed that cutting off the oxygen supply temporarily will switch the steady state to the oscillatory state; the reverse process was accomplished by spiking the reaction system with hydrogen peroxide. Bursting oscillations interrupted by long near-steady-state phases were also observed and are interpreted as switching between the oscillations and steady state either due to experimental fluctuations or to the emergence of a Hopf bifurcation resulting from a change in the NADH concentration.

I. Introduction

The peroxidase–oxidase (PO) reaction is the oxidation of an organic substrate with molecular oxygen as an electron acceptor. The reaction is catalyzed by the enzyme peroxidase and has the following net stoichiometry:

$$2YH_2 + O_2 \rightarrow 2Y + 2H_2O \qquad (1)$$

YH_2 may be one of the following substances: reduced nicotinamide adenine dinucleotide (NADH), indoleacetic acid, dihydroxyfumaric acid, or triose reductone. With NADH, various types of nonlinear behavior have been observed including bistability between two steady states,[1] damped[2] and sustained oscillations,[3] and chaos.[4]

This paper reports our recent observations of the coexistence of sustained periodic oscillations and a stable steady state under certain experimental conditions. This coexistence means that the reaction can go either to a steady state or to periodic oscillations depending on the initial conditions. Furthermore, one can induce the system to transfer from one state to the other through some finite perturbations. This phenomenon has also been described as a bistability between oscillations and a steady state. For brevity, we shall refer to this phenomenon as "O+S bistability" (for *O*scillations plus *S*teady state). Also, throughout the rest of this paper, we will exclusively refer to the PO reaction with NADH as substrate.

A detailed mechanism of the PO reaction that can account for the damped oscillations as well as the bistability between two steady states had been proposed by Aguda and Clarke.[5] This mechanism was further shown by Aguda and Larter[6] to exhibit sustained oscillations as well as O+S bistability. Aguda and Larter also performed computer simulations which predicted that cutting off the oxygen supply temporarily will induce a transition from the steady state to oscillations, an experimental observation we already made in our laboratory prior to the computational results. Furthermore, the computer simulations predicted that the reverse transition from oscillations to steady state can be accomplished by adding sufficient hydrogen peroxide to the reaction mixture. We have tested this prediction in our laboratory and found good qualitative agreement with the numerical results of Aguda and Larter.[6] In addition, we have observed the phenomenon of bursting oscillations interrupted by long near-steady-state phases. It is argued that this phenomenon can be explained by the presence of O+S bistability and that the switching between oscillations and steady state can be due either to experimental fluctuations or to the emergence of a Hopf bifurcation resulting from a change in the NADH concentration.

II. Experimental Section

The reaction vessel we used in our experiments is cylindrical with a circular cross section and is made of polypropylene. The vessel has a lid with holes for the stirrer shaft, inlet and outlet for the flow of a mixture of O_2 and N_2, and for the capillary tube supplying NADH. The temperature is controlled by a thermostatic jacket. Efficient mixing of the reaction mixture is done by a stirrer attached to a high-precision electromotor. Between the surface of the solution and the lid is a 4–5-mL gas headspace containing the mixture of N_2 and O_2. The ratio of this mixture was adjusted by using digital gas mixers as described by Lundsgaard and Degn.[7]

At a constant stirring speed, the diffusion v_t of oxygen across the gas/liquid boundary is described by the equation

$$v_t = k_t([O_2]_{eq} - [O_2]) \qquad (2)$$

where $[O_2]_{eq}$ is the dissolved oxygen concentration at equilibrium between gas and liquid, $[O_2]$ is the oxygen concentration in the liquid, and k_t is the oxygen transfer rate constant. The dissolved oxygen concentration was measured by a Clark-type electrode (Radiometer, Copenhagen, Denmark). To calibrate the reading from this electrode and to measure k_t, dissolved oxygen in the acetate buffer solution placed in the reaction vessel is equilibrated before any of the other reactants are introduced. The magnitude of k_t depends on the surface area of the liquid and hence on the stirring rate. The stirring rate was chosen so that k_t is anywhere between 0.12 and 0.23 min^{-1}. NADH was supplied as a concentrated solution ($\sim$0.1 M) through a capillary tube connected to a high-precision syringe infusion pump (Ole Dich Model 104.SA/107, Copenhagen).

The reaction mixture consisted of 4.5 or 5.0 mL of 0.1 M sodium acetate buffer (pH 5.1) to which were added horseradish peroxidase, 2,4-dichlorophenol (dissolved in 96% ethanol), and methylene blue. A commercial preparation of horseradish peroxidase (HRP) was used in our experiments (Böehringer, Mannheim, Federal Republic of Germany). A stock solution of the enzyme was prepared by dissolving the enzyme in a phosphate buffer (pH 7.0). The 2,4-dichlorophenol and methylene blue were obtained from Merck.

III. Results

The conditions used for the 12 experiments presented in this paper are summarized in Table I and will be described in detail below in conjunction with Figures 1–5. The concentrations in micromolar of the enzyme (HRP), methylene blue (MB), and 2,4-dichlorophenol (DCP) are those in the final reaction mixture. The percentage by volume of the oxygen in the gas headspace of the reaction vessel (column 3 of Table I) is either 1.3% or 2.0%

(1) Degn, H. *Nature* **1968**, *217*, 1047.
(2) Yamazaki, I.; Yokota, K.; Nakajima, R. *Biochem. Biophys. Res. Commun.* **1965**, *21*, 582.
(3) (a) Nakamura, S.; Yokota, K.; Yamazaki, I. *Nature* **1969**, *222*, 794. (b) Olsen, L. F.; Degn, H. *Biochim. Biophys. Acta* **1978**, *523*, 321. (c) Fed'kina, V. R.; Bronnikova, T. V.; Ataullakhanov, F. I. *Stud. Biophys.* **1981**, *82*, 159.
(4) Olsen, L. F.; Degn, H. *Nature* **1977**, *267*, 177.
(5) Aguda, B. D.; Clarke, B. L. *J. Chem. Phys.* **1987**, *87*, 5765.
(6) Aguda, B. D.; Larter, R. Sustained oscillations and bistability in a detailed mechanism of the peroxidase–oxidase reaction. *J. Am. Chem. Soc.* **1990**, *112*, 2167.
(7) Lundsgaard, J.; Degn, H. *IEEE Trans. Biomed. Eng. BME* **1974**, *20*, 384.

0002-7863/90/1512-6652$02.50/0

Table I. Conditions Used for the Experiments Shown in Figures 1–5[a]

figure	[HRP], μM	O_2(g), % (v/v)	NADH, μM/min	[MB], μM	[DCP], μM	temp, °C	k_t, min^{-1}	$k_t[O_2]_{eq}$, μM/min
1a	0.50	2.0	9.3	0.1	20.0	29.0	0.23	5.52
1b	0.47	2.0	10.7	0.2	40.0	28.0	0.23	5.52
1c	0.54	2.0	11.2	0.2	24.0	29.0	0.23	5.52
2a	0.53	1.3	3.8	0.2	21.6	28.0	0.19	2.96
2b	0.53	1.3	3.8	0.2	21.6	28.0	0.14	2.18
2c	0.534	1.3	4.5	0.2	21.6	28.2	0.14	2.18
3	0.53	1.3	4.3	0.2	21.6	28.3	0.14	2.18
4a	0.53	1.3	3.8	0.2	21.6	28.0	0.12	1.87
4b	1.07	1.3	4.3	0.2	10.8	28.2	0.14	2.18
4c	1.07	1.3	4.5	0.2	21.6	28.2	0.14	2.18
4d	0.534	1.3	4.2	0.2	21.6	28.2	0.14	2.18
5	0.50	2.0	9.3	0.2	40.0	29.0	0.23	5.52

[a] Figures 1–3 are cases where coexistence of steady and oscillatory states were observed; Figure 4a–d did not show this coexistence and Figure 5 shows autonomous switching between a steady state and oscillations. All reactions were conducted in an acetate buffer solution of pH 5.1. Abbreviations: HRP, horseradish peroxidase; NADH, reduced nicotinamide adenine dinucleotide; MB, methylene blue; DCP, 2,4-dichlorophenol; k_t, oxygen transfer rate constant; $[O_2]_{eq}$, equilibrium concentration of oxygen in the liquid.

corresponding to $[O_2]_{eq}$ of 15.6 or 24 μM, respectively, at the given temperature. To be able to compare the effects of the oxygen content in the gas headspace and rate of stirring at the same time, the values of $k_t[O_2]_{eq}$, which gives the maximum rate of oxygen diffusion across the gas/liquid boundary, are calculated and are listed in the last column. The flow rate of NADH is reported as the increase in NADH concentration in the solution if NADH had not been consumed (column 4 of Table I).

A. Transition from Steady State to Oscillations. Parts a–c of Figure 1 are examples of experiments in which dissolved oxygen starts from a steady state and the transition to oscillations is accomplished by temporarily cutting off the oxygen supply for 1.5–3 min. (The "wiggles" around the steady state represent electrical noise from the oxygen electrode.) We note that there are two ways that the eventual oscillations in Figure 1 are approached: in parts a and b, the amplitudes of the transient oscillations are smaller than that of the final oscillations; in part c, the transient oscillations have amplitudes that are larger. The steady state of oxygen in each case is between the maximum and minimum of the oscillations.

B. Transition from Oscillations to Steady State. Under certain conditions, an oscillating PO reaction can be induced to a steady state by spiking the reaction mixture with H_2O_2 as demonstrated in Figure 2a–c. Immediately after the introduction of H_2O_2 (as indicated by the arrows in the figure), oxygen is rapidly consumed. In Figure 2, H_2O_2 was introduced when the oxygen oscillation had almost reached its minimum. Three different ways that a steady state can be obtained from oscillations are shown. In Figure 2a, the steady state is approached from below in a damped oscillatory manner. In Figure 2b, oxygen first increases beyond the maximum of the oscillations and then decreases monotonically to the steady state; Figure 2c is similar to the latter except that now the steady state is approached through damped oscillations. Again, in all three cases shown in Figure 2, the steady state is located between the maximum and minimum of the oscillations.

C. Reversible Switching between Steady State and Oscillations. A further experimental proof of O+S bistability is to show that a transition between oscillations and steady state is reversible. Such an experiment is shown in Figure 3. Oscillations are first obtained and the transition to a steady state is accomplished by the addition of H_2O_2. The steady state is then perturbed by cutting off the oxygen supply temporarily and the reaction returns to sustained oscillations.

D. Conditions for the Coexistence of Steady State and Oscillations. It was generally observed in all our experiments (including those that are not reported here) that O+S bistability occurs when the enzyme concentration is low, typically around 0.5 μM. As demonstrated by the pair of experiments in Figures 2c and 4c with identical conditions except for the enzyme concentration, a decrease in [HRP] from 1.07 to 0.534 μM leads to O+S bistability.

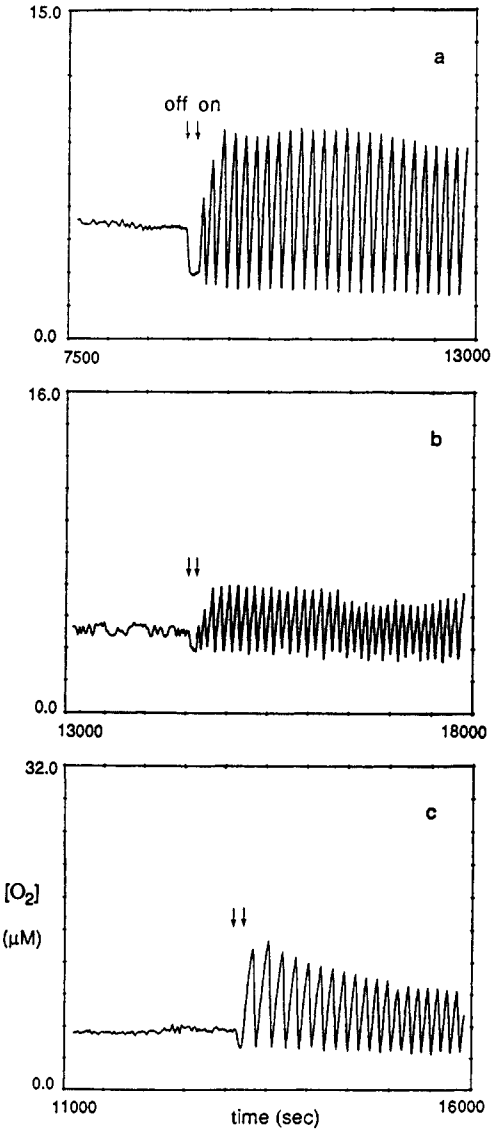

Figure 1. Experiments showing transitions from steady state to oscillations induced by cutting off the oxygen supply temporarily (indicated by the pair of off/on arrows). The "wiggles" around the steady states are due to electrical noise from the oxygen electrode. Experimental conditions are given in Table I.

The infusion rate of NADH and stirring rate were also observed to be critical. The experiments in Figures 2c and 4d differ only in the NADH flow rate; under the conditions of this pair of

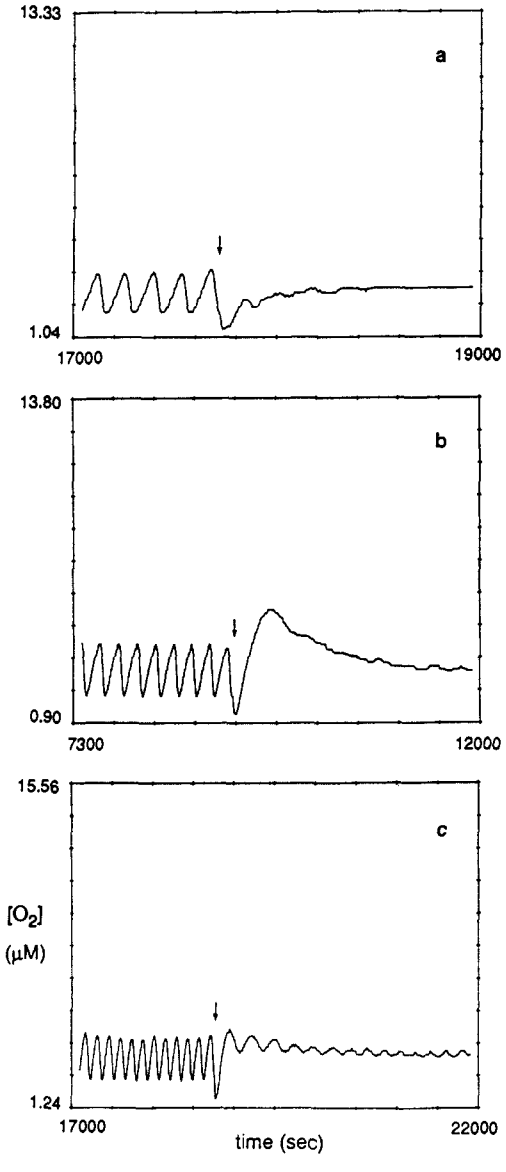

Figure 2. Experiments showing transitions from oscillations to steady state accomplished by spiking the reaction mixture with hydrogen peroxide at the times indicated by the arrows. The volumes (in microliters) and concentrations (in millimolar) of the stock H_2O_2 solution used in the perturbations are as follows: (a) 15 μL, 1.8 mM; (b) 20 μL, 1.8 mM; (c) 15 μL, 2 mM. Other experimental conditions are given in Table I.

experiments, an increase in NADH flow rate from 4.2 to 4.5 μM/min led to the occurrence of O+S bistability. The effect of the stirring rate is clearly shown in the experiments of Figures 2b and 4a; an increase in k_1 from 0.12 to 0.14 min^{-1} led to O+S bistability. Lastly, we note that the occurrence of O+S bistability is not sensitive to the concentrations of methylene blue and 2,4-dichlorophenol as demonstrated by the experiments of Figure 1a and b.

The H_2O_2 perturbations in Figure 4a–d indicate that the oscillatory state is the only stable state. With the experimental conditions used in Figure 4a, the addition of H_2O_2 damps the oscillations momentarily but the amplitudes of the oscillations increase and return to sustained oscillations. In Figure 4b, immediately after the addition of H_2O_2, oxygen is consumed rapidly but soon afterward increases beyond the maximum of the original oscillations and then the amplitude decreases back to the original oscillations. The case of Figure 4c can be described as a mixture of Figure 4a and b. Finally, Figure 4d looks very similar to Figure 2c except this time in 4d, instead of settling down to a steady state, sustained oscillations are obtained.

E. Autonomous Switching between Oscillations and Steady State. Figure 5 is an experiment performed under conditions that

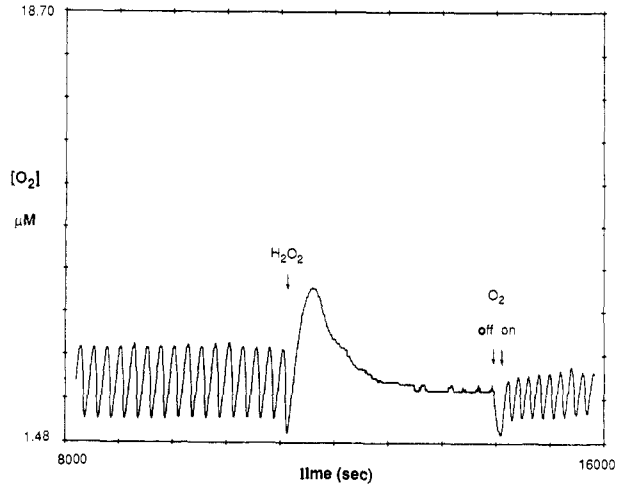

Figure 3. An experimental run showing the reversibility of the transition from oscillations to steady state. Experimental conditions are given in Table I. The oscillations were first perturbed with 20 μL of 1.8 mM H_2O_2 stock solution (indicated by the first arrow on the left). The reaction has settled down to stable steady state for at least 0.5 h before the oxygen supply was cut off temporarily (indicated by the pair of off/on arrows on the right) to return the reaction to the oscillatory state.

are very near those of Figure 1b where O+S bistability was observed earlier. In Figure 5, a near-steady state gave way to oscillations that lasted for almost 2 h, after which a "steady-state" phase (no oscillations but a very slow increase in oxygen) occurred for ~2 h. The oscillations suddenly reappeared after oxygen had reached the same level as when the first oscillations came about. On the basis of previous experiments where we measured [NADH] spectrophotometrically, we believe that the slow increase in $[O_2]$ during the near-steady-state phase (Figure 5) is accompanied by a decrease in the average level of [NADH]. It will be argued in the final section of this paper that, in the case of Figure 5, a steady state and an oscillatory state coexist and the switching between these states can be induced by experimental fluctuations or by a change in the NADH concentration.

IV. Discussion

The results presented here have demonstrated the coexistence of sustained oscillations and stable steady state (or O+S bistability) in the PO reaction under certain conditions. We have also shown that a transition from the steady state to oscillations is accomplished by cutting off the oxygen supply temporarily. The reverse transition was induced by spiking the reaction mixture with hydrogen peroxide. The experiments on H_2O_2 perturbations were performed to check the theoretical predictions of Aguda and Larter[6] based on a detailed mechanism called model A proposed earlier by Aguda and Clarke.[5] This model predicted O+S bistability as well as the transition from steady state to oscillations by cutting off the oxygen supply temporarily. Model A assumes that NADH concentration is kept constant, which, experimentally, would require either a large reservoir of NADH or a varying infusion rate of NADH to offset its consumption by certain reactions in the mechanism. In every experiment we conducted, the NADH infusion rate was constant and we observed oscillations of NADH along with oxygen oscillations.

As can be seen from Aguda and Larter's Figure 7, O+S bistability exists when there are three steady states: for oxygen, the lowest steady state is locally stable, the middle is an unstable saddle point, and the largest steady state has undergone a Hopf bifurcation to a limit cycle. In Figure 8 of Aguda and Larter's paper, the steady state of oxygen is not located between the maximum and minimum of the oxygen oscillations. Thus, there are qualitative and quantitative differences between model A and experiment. These differences, nevertheless, do not preclude the possibility of multiple steady states in the experimental system as shown below.

A PO reaction system having three steady states and an oxygen time series like the experiments can have phase portraits whose

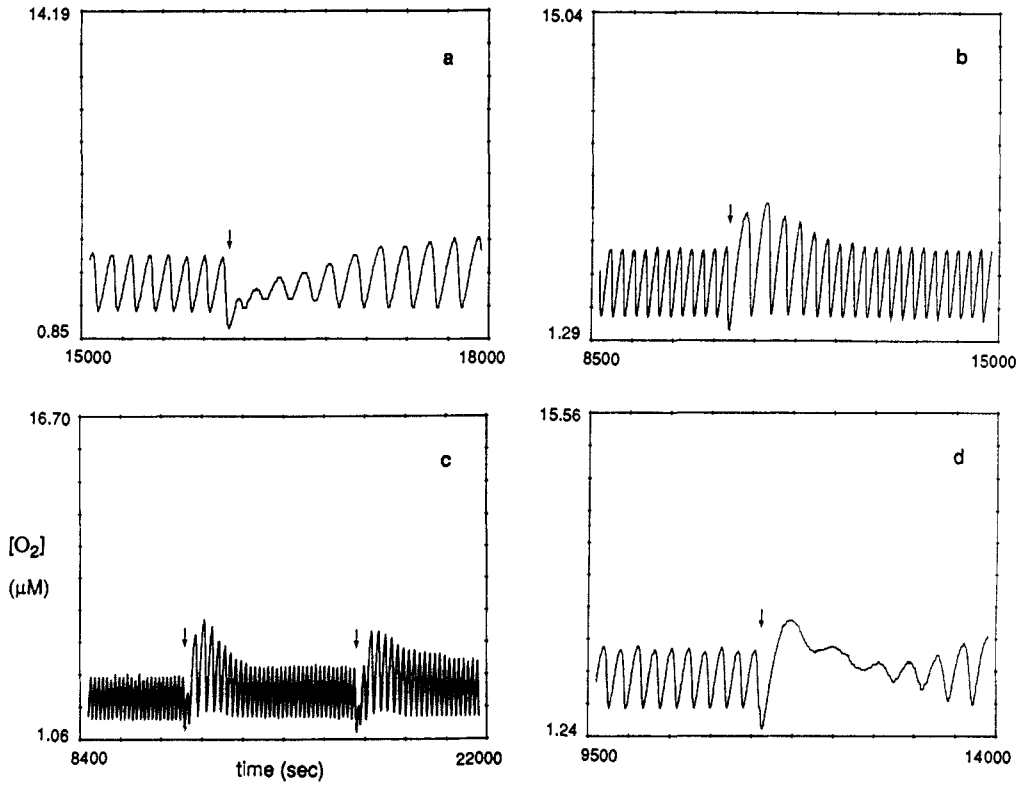

Figure 4. Experiments where H_2O_2 perturbations did not lead to a transition from oscillations to steady state. The amounts and concentrations of the stock H_2O_2 solution used in the perturbations are as follows: (a) 20 μL, 1.8 mM; (b) 15 μL, 2 mM; (c) 5 (left arrow) and 20 μL (right arrow), 2 mM; (d) 20 μL, 2 mM. Other experimental conditions are given in Table I.

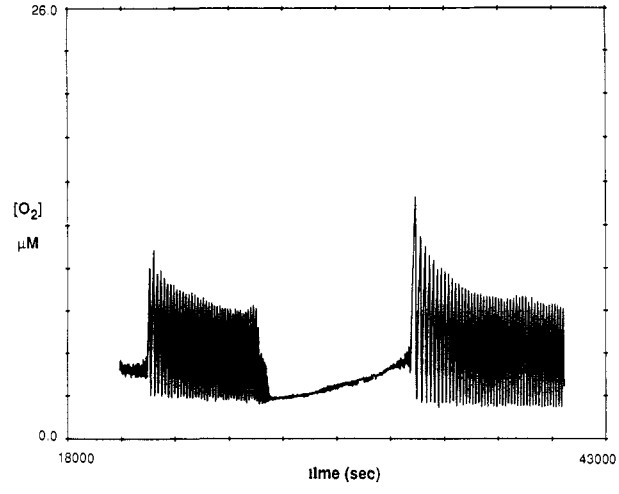

Figure 5. Autonomous switching of the reaction between oscillations and a near-steady-state phase. Experimental conditions are given in Table I.

two-dimensional projections are shown in Figure 6a on the $[O_2]$–$[H_2O_2]$ plane. However, the two-dimensional projection of the phase portrait shown in Figure 6b can also explain the experiments. In Figure 6b, we assume the existence of an unstable periodic orbit around a locally stable steady state. The unstable cycle is surrounded by a limit cycle. Thus we have a situation where there is a unique steady state and an O+S bistability exists. At this time, we cannot discriminate the two possibilities presented in Figure 6 (not to mention other more complicated scenarios that are possible because of the high mathematical dimension of the dynamical system). All the oxygen time series presented for the O_2 and H_2O_2 perturbations can be accounted for by the two scenarios in Figure 6. (We emphasize that a third dimension in the phase portrait would be needed to account for those time series shown in Figure 4.) The bursting oscillations can be explained by Figure 6a when the periodic orbit visits the saddle point very

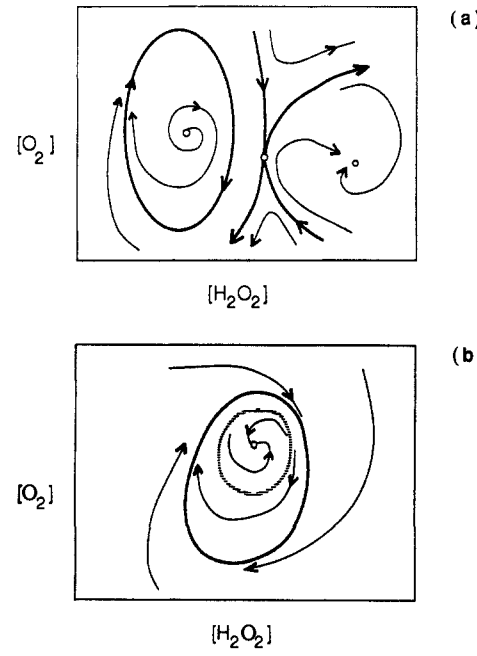

Figure 6. Hypothetical phase portraits of the reaction dynamics *projected* on the $[O_2]$–$[H_2O_2]$ plane that can account for the experimental time series shown in Figures 1–3 and Figure 5: (a) coexistence of a limit cycle and a stable steady state in a multiple-steady-state situation; (b) coexistence of a limit cycle and a locally stable steady state in a unique-steady-state situation—the basins of attraction of the two attracting states are separated by an unstable periodic orbit.

closely where the trajectory slows down (giving the appearance of a steady state). On the other hand, the case of Figure 6b can explain bursting if the stable limit cycle and unstable cycle are almost "touching" each other at some regions so that experimental fluctuations can switch the system between oscillations and steady state.

Lastly, the observed increase in $[O_2]$ during the "steady-state" phase in Figure 5 is believed to be accompanied by a decrease in the NADH concentration. In the context of model A, this change in [NADH] implies changing the values of the pseudo rate constants used for certain reactions where NADH is involved. This could destabilize a steady state and lead to oscillations after [NADH] has decreased below a critical level.

Acknowledgment. This research was supported by the Danish Natural Science Research Council.

Registry No. NADH, 58-68-4; O_2, 7782-44-7; H_2O_2, 7722-84-1; peroxidase, 9003-99-0.

A Secondary $^{11}C/^{14}C$ Kinetic Isotope Effect in the Base-Catalyzed Prototropic Rearrangement of 1- to 3-Methylindene

B. Svante Axelsson, Kjell-Åke Engdahl, Bengt Långström, and Olle Matsson*

Contribution from the Department of Organic Chemistry, Institute of Chemistry, Uppsala University, P.O. Box 531, 721 21 Uppsala, Sweden. *Received December 19, 1989*

Abstract: The secondary $^{11}C/^{14}C$ kinetic isotope effect (KIE) has been determined to 1.010 ± 0.005 for the base-catalyzed rearrangement of 1-methylindene (**1**) to 3-methylindene (**2**) isotopically substituted in the methyl group in the solvent benzene at 20 °C by using the tertiary amine DABCO as catalyst. The result is discussed in connection with previously reported values of the corresponding primary ^2H and secondary β-$^2H_3$ KIEs (5.03 and 1.103, respectively). The isotope effects are consistent with a late TS, structurally close to the ion-pair intermediate postulated in the rate-determining proton abstraction step of the reaction. The influence of hyperconjugation and rehybridization on the magnitude of the secondary carbon KIE is discussed.

Introduction

Kinetic isotope effects (KIEs) provide one of the most powerful tools in the elucidation of reaction mechanisms and transition-state structures.[1] KIEs obtained by isotopic substitution at several positions in a reacting system (successive labeling) are especially useful, particularly in combination with theoretical model calculations.

Heavy element isotope effects are relatively small in magnitude, e.g., primary $^{12}C/^{14}C$ isotope effects are usually less than 16%.[1] Recently the $^{11}C/^{14}C$ kinetic isotope effect method was presented.[2] This was the first reported application of ^{11}C in isotope effect studies. In the determination of $^{11}C/^{14}C$ KIEs a large mass range of carbon isotopes is utilized, and the $^{11}C/^{14}C$ KIE method might thus be suitable for measurements of small effects such as secondary isotope effects. ^{11}C is an accelerator-produced positron emitting radionuclide with a half-life of 20.34 min. The $^{11}C/^{14}C$ KIE method[3] is based on HPLC fractionation of the labeled reactants and products of the reaction and subsequent radioactivity measurements of ^{11}C and ^{14}C in these fractions as determined by liquid scintillation counting.

Indene and alkylindenes were found to be useful substrates early on for the study of base-catalyzed proton-transfer reactions; a new feature being the first discovery of intramolecular and stereospecific isomerization (with suprafacial shift of the proton), under suitable circumstances, when amines were used as catalysts.[4] As expected, KIEs[5] and enantioselectivity[6] were observed. We have recently reported comprehensive KIE studies by using modern techniques[7,9] and, to the best of our knowledge, the first example of an enantiomer-dependent KIE in an asymmetric catalytic reaction.[8]

Scheme I

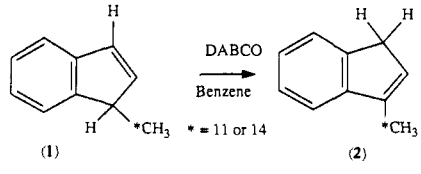

(1) (2)

For the base-catalyzed prototropic rearrangement of 1-methylindene to 3-methylindene the primary deuterium KIE was determined to 5.03 ± 0.06 in toluene at 20 °C by using 1,4-diazabicyclo[2.2.2]octane (DABCO) as the base[7a] (deuterium was substituted for hydrogen in the 1- and 3-positions). The secondary β-deuterium KIE for the same reaction (deuterium substitution in the methyl group; $-CD_3$) was determined to 1.103 ± 0.001, in toluene at 20 °C.[7a]

In this paper the secondary $^{11}C/^{14}C$ KIE for the prototropic rearrangement of 1- to 3-methylindene, catalyzed by DABCO in benzene at 20 °C, see Scheme I, is presented.

Three KIEs, with the isotopic substitution in different positions, have thus been determined for the same reaction. Taken together, these isotope effects yield information on the structure of the TS with regard to its position along the reaction coordinate. Moreover, the methyl KIEs may be used to probe the degree of electronic charge localization on the carbon atom from which the proton is abstracted.

Theoretical model calculations of KIEs for the present reaction, with use of the semiclassical BEBOVIB IV program,[10] are in progress and will be reported in a forthcoming paper.[11] Some of the results

(1) Melander, L.; Saunders, W. H., Jr. *Reaction Rates of Isotopic Molecules*; John Wiley and Sons: New York, 1980.
(2) Axelsson, B. S.; Långström, B.; Matsson, O. *J. Am. Chem. Soc.* **1987**, *107*, 7233.
(3) Axelsson, B. S.; Matsson, O.; Långström, B. *J. Phys. Org. Chem.* In press.
(4) Bergson, G.; Weidler, A.-M. *Acta Chem. Scand.* **1963**, *17*, 1798.
(5) Bergson, G.; Weidler, A.-M. *Ibid.* **1964**, *18*, 1498.
(6) Ohlsson, L.; Wallmark, I.; Bergson, G. *Ibid.* **1966**, *20*, 750.
(7) (a) Matsson, O. *J. Chem. Soc., Perkin Trans. II* **1985**, 221. (b) Hussénius, A.; Matsson, O.; Bergson, G. *Ibid.* **1989**, 851.
(8) Matsson, O.; Meurling, L.; Obenius, U.; Bergson, G. *J. Chem. Soc., Chem. Commun.* **1984**, 43.
(9) Bergson, G.; Matsson, O.; Sjöberg, S. *Chem. Scr.* **1977**, *11*, 25.
(10) Sims, L. B.; Burton, G.; Lewis, D. E. BEBOVIB IV, *Quantum Chemistry Program Exchange*, 1977; Program No. 337, Department of Chemistry, Indiana University, Bloomington, IN 47401.

0002-7863/90/1512-6656$02.50/0